Article

Organization of Endothelial Cells, Pericytes, and Astrocytes into a 3D Microfluidic in vitro Model of the Blood-Brain Barrier

Jack D. Wang, El-Sayed Khafagy, K M Khanafer, Shuichi Takayama, and Mohamed E.H. El-Sayed

Mol. Pharmaceutics, **Just Accepted Manuscript** • DOI: 10.1021/acs.molpharmaceut.5b00805 • Publication Date (Web): 10 Jan 2016

Organization of Endothelial Cells, Pericytes, and Astrocytes into a 3D Microfluidic *in vitro* Model of the Blood-Brain Barrier

Jack D. Wang[a], El-Sayed Khafagy[a,b], Khalil Khanafer[a], Shuichi Takayama[a,c,] and Mohamed ElSayed[a,c,*]

[a]University of Michigan, Department of Biomedical Engineering, 1101 Beal Avenue, Ann Arbor, Michigan, 48109, USA

[b]Department of Pharmaceutics and Industrial Pharmacy, Faculty of Pharmacy, Suez Canal University, Ismailia 415-22, Egypt

[c]University of Michigan, Macromolecular Science and Engineering Program, 2300 Hayward Avenue, Ann Arbor, Michigan, 48109, USA

*Corresponding Author:

Mohamed E.H. ElSayed, Ph.D.

University of Michigan

Department of Biomedical Engineering

1101 Beal Avenue

Lurie Biomedical Engineering Building, Room 2150

Ann Arbor, MI 48109

USA

Phone: +1 (734) 615-9404

Fax: +1 (734) 647-4834

E-mail: melsayed@umich.edu

Web: www.bme.umich.edu/centlab.php

Table of Contents Graphic

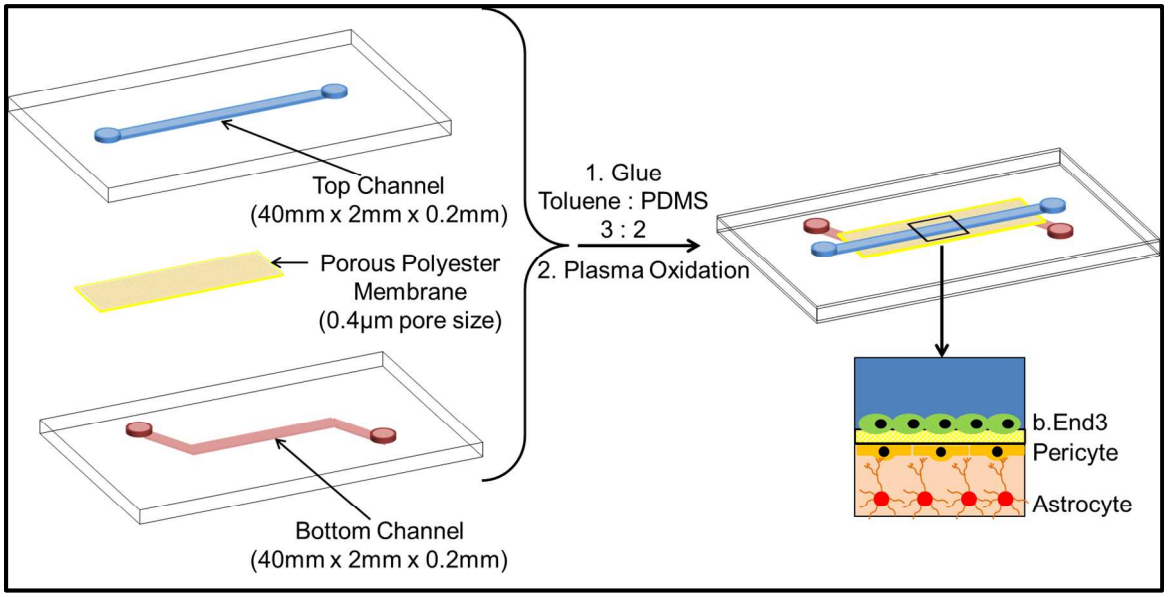

Abstract

The endothelial cells lining the capillaries supplying the brain with oxygen and nutrients form a formidable barrier known as the blood-brain barrier (BBB), which exhibits selective permeability to small drug molecules and virtually impermeable to macromolecular therapeutics. Current *in vitro* BBB models fail to replicate this restrictive behavior due to poor integration of the endothelial cells with supporting cells (pericytes and astrocytes) following the correct anatomical organization observed *in vivo*. We report the co-culture of mouse brain microvascular endothelial cells (b.End3) and pericytes +/- C8-D1A astrocytes in layered microfluidic channels forming three dimensional (3D) bi- and tri-culture models of the BBB. The live/dead assay indicated high viability of all cultured cells up to 21 days. Trans-endothelial electrical resistance (TEER) values confirmed the formation of intact monolayers after 3 days in culture and showed statistically higher values for the tri-culture model compared to the single and bi-culture models. Screening the permeability of [14C]-mannitol and [14C]-urea showed the ability of bi- and tri-culture models to discriminate between different markers based on their size. Further, permeability of [14C]-mannitol across the tri-culture model after 18 days in culture matched its reported permeability across the BBB *in vivo*. Mathematical calculations also showed that the radius of the tight junctions pores (R) in the tri-culture model is similar to the reported diameter of the BBB *in vivo*. Finally, both the bi- and tri-culture models exhibited functional expression of the P-glycoprotein efflux pump, which increased with the increase in the number of days in culture. These results collectively indicate that the tri-culture model is a robust *in vitro* model of the BBB.

Keywords: Blood-brain barrier, layered microfluidic channels, 3D *in vitro* models, b.End3 endothelial cells, C8-D1A astrocytes, Co-culture systems.

Introduction

The endothelial cells lining the capillaries that supply the brain with oxygen and nutrients present a highly regulated barrier known as the blood-brain barrier (BBB)[1, 2]. These endothelial cells are characterized by thick cell membranes, few endocytic vesicles, absence of fenestrae, and highly organized tight junctions that restrict molecular diffusion across the paracellular space **(Figure 1)**[1, 2]. The endothelial cells along with other supporting cells such as, neurons[1], pericytes[2], astrocytes[3], and microglial cells[1] control the integrity of the BBB and are collectively known as the neurovascular unit[3]. The integrity and function of the BBB is regulated by several environmental factors including flow-induced shear stress[1], endothelial cell-to-cell contact[1, 3], communication within the neurovascular unit[1], and the local concentration of secreted chemical factors[3]. As a result of the restrictive nature of the BBB, only 2% of small molecular weight (< 500 Daltons) drugs permeate across the BBB and achieve therapeutic concentrations in the brain[4]. Further, large molecular weight drugs (e.g. peptides, proteins, and nano-medicines) generally cannot diffuse across the BBB[1, 2]. Consequently, treatment of several neurological disorders such as Alzheimer disease, Huntington disease, stroke, and brain cancer is limited by the lack of new drug molecules that can effectively permeate across the BBB and achieve the desired therapeutic concentration in diseased brain cells[4].

There is a significant interest in the development of *in vitro* models of the BBB that replicate the organization and restrictive behavior observed *in vivo*, which will allow their use for non-invasive, rapid, economic, and reproducible screening of the BBB permeability of new drug candidates. Static *in vitro* models of the BBB have been developed by culturing endothelial cells from different sources (e.g. human[5], porcine[6], or

immortalized cell lines[7]) alone or in combination with supporting cells (pericytes[5], astrocytes[8], or neurons[6]) on a semipermeable membrane in the transwells setup[6]. Unfortunately, these models exhibit low trans-endothelial electrical resistance (TEER)[6], high permeability of typically impermeable marker molecules[6], low expression and functionality of transporters (e.g. the P-glycoprotein efflux pump)[6], and short term viability[1], which dramatically limit their value as a screening tool to determine the likelihood that a potentially therapeutic molecule can permeate from the systemic circulation, across the BBB, and into the brain.

To address the limitations of static models, the dynamic *in vitro* BBB (DIV-BBB) model was developed by culturing endothelial cells and astrocytes on the inside and outside wall of hollow fibers, respectively[9]. Pulsatile flow of the culture medium through the hollow fibers was used to exert shear stress on the surface of the endothelial cells, which proved to increase the expression of the tight junction proteins and enhance barrier integrity[9]. However, formation of a restrictive endothelial cell monolayer takes a long time (9-12 days) as indicated by the time it took for TEER values to stabilize at its maximum value. In addition, the thickness (150μm) of the fibers' wall used in this device is significantly higher than the thickness (10μm) of the porous membrane of conventional transwells, which reduce endothelial cell-to-pericytes contact[10]. Recently, two microfluidic devices have been used to develop *in vitro* models of the BBB that incorporate flow-mediated shear stress on cultured endothelial cells. Kim and co-workers described the use of microfluidic channels (200μm high, 2mm luminal width, and 5mm abluminal width), which incorporated multiple electrodes to monitor TEER using glass support where they co-cultured endothelial cells and astrocytes on the opposite sides of a

porous membrane (membrane thickness = 10μm; pore size = 0.4μm)[10]. The microfluidic device was connected to a pump to achieve a flow rate of 2.6 μl/min of the culture medium in the top channel, which exerted shear stress of 1.6 dyne/cm^2 on the cultured endothelial cells. Incorporating shear stress in this model increased TEER values across the cultured monolayer compared to that established in microfluidic devices under static conditions. However, there was no significant difference in TEER or size selectivity of BBB models established by endothelial cells alone or in combination with the astrocytes in this device despite of the applied shear stress. Prabhakarpandian and co-workers described the Sym-BBB model, which is a plastic and optically clear microfluidic chip that enables microcirculation in a side-by-side two compartment chamber. The side-by-side two compartment configuration allowed co-culture of endothelial cells and supporting neural cells coupled with circulation of astrocytes-conditioned medium (ACM) in the abluminal compartment, which enhanced the expression of the tight junction proteins between cultured endothelial cells[11].

Unfortunately, these microfluidic BBB models fail to accurately replicate the organization of the neurovascular unit or the associated restrictive behavior observed *in vivo*. Specifically, in the first device, the endothelial cells and astrocytes are cultured on opposite sides of the porous membrane, which does not match the anatomical organization of the capillaries supplying the brain[3]. Endothelial cells are actually sheathed by pericytes (smooth muscle cells), which play a critical role in maintaining the integrity of the capillary structure and enhancing barrier properties of the endothelial cells[12-15]. Earlier reports show that communication between co-cultured endothelial cells and astrocytes rely on secreted soluble factors to enhance barrier properties of the

established monolayers[1, 3, 8]. This is confirmed by the lack of a statistically significant difference in the permeability of marker molecules across the monolayers of endothelial cells alone or those co-cultured with astrocytes[10]. There is also limited information about the viability span of the co-culture system as TEER results were reported for only 4 days, which is the time it took for the monolayer to reach maximum TEER values[10]. Further, there is no information about the functional expression of key transporters such as the P-glycoprotein efflux pump, which has been shown to limit the transport of chemotherapeutic agents across the BBB *in vivo*[16]. Despite the easy manufacturing of the second device and the ability to visually confirm the development of the tight junction in the cultured endothelial cells, absence of supporting cells such as pericytes and astrocytes reduce the restrictiveness of the formed barrier compared to *in vivo* conditions.

We address the limitations of earlier microfluidic BBB models by co-culturing mouse brain endothelial cells (b.End3) with pericytes and astrocytes in layered microfluidic devices following the same organization of the neurovascular unit observed *in vivo* to develop a three-dimensional (3D) *in vitro* BBB model that successfully mimics the restrictive transport properties observed *in vivo*. Our device is composed of layered microfluidic channels (W = 2mm; L = 4cm; H = 200μm) sandwiching a porous membrane (0.4μm pore size) fabricated using soft lithography[17, 18]. We embedded Ag/AgCl electrodes in the upper and lower microfluidic PDMS channels to allow real time measurement of TEER across cultured endothelial cells[18]. We cultured b.End3 endothelial cells and mouse pericytes on opposite sides of a porous membrane (pore size = 0.4μm) with a 10μm thickness to establish a bi-culture model that mimics their natural organization *in vivo*. We cultured mouse astrocytes on the bottom of the lower channel to

develop the tri-culture model **(Figure 2A)**. We measured TEER and investigated the permeability of mannitol (MW = 182 g/mol) and urea (MW = 60 g/mol) across bi- and tri-culture models to determine the effect of co-culturing b.End3 cells with pericytes and astrocytes on the integrity of the formed barriers. Using the permeability data of mannitol and urea to solve the equation of the Renkin function (a dimensionless molecular sieving function for cylindrical channels comparing comparing the molecular radius (r) with the pore radius (R) where $0 < F(r/R) < 1.0$), we also calculated the size of the tight junction pores in bi- and tri-culture models. We gradually increased the height of the lower microfluidic channel from 200 μm to 600 μm and 1,000 μm in the tri-culture model while keeping all other experimental conditions constant to investigate the effect of distance between the cultured astrocytes and bEnd.3/pericytes monolayer on the "restrictiveness" of the formed barrier. Finally, we investigated the apical-to-basolateral (AB) and basolateral-to-apical (BA) permeability of dexamethasone, a known substrate of the P-glycoprotein (P-gp) efflux pump, across bi- and tri-culture models to measure functional expression of the P-gp pump as a function of days in culture.

Experimental Section

Materials

Poly(dimethylsiloxane) (Sylgard 184) was purchased from Dow Corning (Midland, MI). SU-850 was purchased from MicroChem (Newton, MA). Toluene and sterile fibronectin solution were purchased from Sigma-Aldrich (St. Louis, MO). [14C]-D-mannitol (100 μCi/ml) and [14C]-urea (100 μCi/ml) were purchased from Moravek Biochemicals and Radiochemicals (Brea, CA). [3H]-Dexamethasone (1 mCi/ml) was

purchased from American Radiolabeled Chemicals, Inc. (St. Louis, MO). Mouse brain endothelial cells (b.End3) and Astrocyte type I clone (C8-D1A) were purchased from ATCC (Manassas, VA). Mouse pericytes were generously gifted by Dr. Anuska Andjelkovic of the University of Michigan. Dulbecco's modified eagle medium, fetal bovine serum, 0.05% trypsin, non-essential amino acids, and live/dead cytotoxicity kits were purchased from Invitrogen Life Technologies Corporation (Carlsbad, CA). Interferon-gamma was purchased from R&D Systems (Minneapolis, MN).

Design and Fabrication of Microfluidic Devices

The microfluidic devices used for culture of b.End3 cells are composed of two layered microfluidic channels (W = 2mm; L = 4cm; H = 0.2, 0.6, or 1mm) sandwiching a porous membrane (0.4μm pore size), which were fabricated using soft lithography following established protocols[17, 18]. Briefly, PDMS prepolymer was mixed with the curing agent at a 10 (prepolymer) / 1 (curing agent) weight ratio before casting onto two 4 inch silicon wafers containing a 200 μm thick positive relief pattern. The mixture was cured at 60 °C for 2 hours before peeling the PDMS layer off the silicon wafer. Access holes were punched with a 16 gauge blunt syringe (1.65 mm outer diameter) forming the inlet and outlet holes for each channel. We spun coated a PDMS/toluene mixture prepared at a 3/2 weight ratio on a clean glass slide for 1 minute to generate a thin mortar layer, which was used to glue the top and bottom PDMS layers. Ag/AgCl recording electrodes were embedded in 500 μm x 500 μm side channels when fabricating microfluidic devices for measurement of TEER across b.End3 monolayers following a published procedure.[18] Polyester membranes with an average pore size of 400 nm were

sandwiched between the aligned top and bottom PDMS channels and glued together before curing for 1 hour until the PDMS mortar completely hardened. Pipette tips (100 µl) were inserted into the inlets and outlets of the top and bottom channels to serve as medium reservoirs before exposure to plasma oxygen for 5 minutes. Sterile fibronectin solution (25 µg/ml) was loaded into the top PDMS channel for 24 hours to coat the polyester membrane followed by exposure of the microfluidic device to UV radiation for sterilization before seeding of b.End3 and mouse pericyte cells.

Cell Culture

Mouse brain endothelial cells (b.End3) were thawed at 37 °C before mixing with 3 mL of culture medium, centrifuging at 1,000 rpm for 3 minutes, aspirating the supernatant, suspending the cell pellet in 10 mL of culture medium, transferring cell suspension to a T75 flask, and incubating the cells in a humidified 5% CO_2 incubator at 37 °C while changing the culture medium every 48 hours. Cultured b.End3 cells were passaged after reaching 80% confluence by incubating with 5mL of 0.05% Trypsin-EDTA solution for 3 minutes at 37°C to collect the cell pellet for splitting into new T75 flasks or seeding onto fibronectin-coated membranes in microfluidic devices at a seeding density of 270 cells/mm^2. Mouse astrocyte type I clone (C8-D1A) were cultured in T75 flasks under the same culture conditions using Dulbecco's Modified Eagle's Medium with 10% FBS following ATCC's culture protocol.

Immortalized mouse pericytes were thawed at 37 °C and directly seeded into T75 flasks that were incubated in a humidified 5% CO_2 incubator at 31°C while changing the culture medium every 24 hours. Cultured pericytes were passaged after reaching 80%

confluence by incubating with 3 mL of 0.05% Trypsin-EDTA solution for 5 minutes at 31°C to collect the cell pellet before splitting into new T75 flasks or seeding in the microfluidic devices at a seeding density of 100 cells/mm^2.

Single culture model refers to the culture of b.End3 cells in the top channel on the fibronectin-coated membrane. To establish the bi-culture model, pericytes were loaded in the bottom channel directly before flipping the microfluidic device upside-down to allow the pericytes to adhere to the fibronectin-coated porous membrane. After 2 hours, the microfluidic devices were inverted back to their normal position and b.End3 cells are seeded in the top channel, which allows the pericytes and bEnd.3 cells to connect through the pores of the supporting membrane. We followed the same sequence for culturing the pericytes and bEnd.3 cells on opposite sides of the porous membrane and allow 24 hours of incubation before adding the astrocytes to the lower channel to develop the tri-culture model. The medium used for culture of pericytes and astrocytes in the bottom channel is standard Dulbecco's Modified Eagle's Medium supplemented with 10% FBS, 5ml of non-essential amino acids, and 8.5µl of Interferon-γ while b.End3 cells in the top channel were cultured in the standard Dulbecco's Modified Eagle's Medium supplemented with 10% FBS. Single, bi-, and tri-culture models are static models with no medium flow-mediated shear stress applied to the cultured endothelial cells. The medium in both top and bottom channels was changed every 6 hours to ensure sufficient supply of nutrients to cultured cells.

Assessment of Cell Viability

Endothelial b.End3 cells, mouse pericytes, and astrocytes cultured in layered microfluidic channels were stained using the live/dead cytotoxicity kit (Life Technologies Corporation, Carlsbad, CA) following manufacturer's protocol. Briefly, 1 µL calcein AM and 1µL ethidium homodimer-1 were added to 1mL of the culture medium before adding 16µL of this mixture to b.End3 cells cultured in the top channel and incubating for 20 minutes at 37ºC under normal culture conditions. Live b.End3 cells, pericytes, and astrocytes were stained green while dead cells were stained red and both were visualized using an inverted fluorescent microscope (Nikon, New York, NY) at 500 nm and 600 nm, respectively. Number of live and dead b.End3 cells observed at the inlet, center, and outlet of the top microfluidic channel was counted in the fluorescent images (1.7mm x 0.88mm) captured at a 10X magnification.

The angle (θ) between cultured b.End3 cells and the longitudinal (X) axis of the top channel in captured fluorescent images (10X magnification) was measured using Photoshop CS4 (Adobe, San Jose, CA) to determine the change in alignment of cell spindle as a function of culture time. The variance of the angle measurements was calculated using equation (1) where σ^2 is the variance, *N* is the number of data points, xi is each specific data point, and µ is the mean:

$$\sigma^2 = \frac{1}{N}\sum_{i=1}^{N}(x_i - \mu)^2$$ ---------- Equation 1

Measurement of TEER across b.End3 Cell Monolayers

Trans-endothelial electrical resistance (TEER) of confluent b.End3 cell monolayers cultured in layered microfluidic channels was measured on daily basis following our published protocol.[18] Briefly, impedance spectra were taken using an autolab

potentiostat/galvanostat at 0.1V of alternating current passing between the two embedded electrodes within layered microfluidic channels. Frequency range between 10 Hz to 1.00 MHz was used to yield a total of 64 impedance measurements. The control impedance spectra measured before seeding the cells were subtracted from the measured impedance spectra with b.End3 cells alone (single culture) or with pericytes (bi- and tri-culture model) to eliminate their contribution to the calculated resistance. We developed a MATLAB code (MathWorks Inc., Natick, MA) using its optimization toolbox to resolve the TEER values, which were normalized to the surface area of the b.End3 monolayers to calculate the resistance in $\Omega.cm^2$.

Paracellular Permeability Across b.End3 Cell Monolayers

We investigated the transport of two paracellular permeability markers namely [14C]-mannitol (182 Da, 11.32μM) and [14C]-urea (60 Da, 353μM) across b.End3 monolayers in single-, bi-, and tri-culture models in layered microfluidic devices after 3, 6, 9, 12, 15, 18, and 21 days of their culture. Briefly, the culture medium was removed from the apical (top) and basolateral (bottom) channels before washing the b.End3 monolayers twice with a warm (37°C) PBS solution prior to starting the transport study. The PBS solution in the apical compartment was replaced with the solution of different markers before incubating the microfluidic devices at 37°C, 95% relative humidity, and 5% CO_2 for 60 minutes. The PBS solution in the receiver compartment (lower channel) of the microfluidic device was collected and replaced with fresh PBS every 10 minutes for 60 minutes. At the end of the 1 hour incubation time, PBS solutions in both the top and bottom channels were collected, mixed with 5mL of the liquid scintillation fluid (GMI

Inc., Ramsey, MN), and analyzed using the Beckman LS6500 Liquid Scintillation Counter (Beckman Coulter Inc., Brea, CA) to determine the concentration of each marker using a standard calibration curve.

The permeability of each marker molecule across b.End3 monolayers was calculated using the following differential equation derived from Fick's Law[9]:

$$P = \frac{V_{basolateral} \times \frac{\Delta C_{basolateral}}{\Delta t}}{A \times C_{apical}}$$ ---------- Equation 2

Where P denotes solute permeability (cm/sec), V is the PBS volume in the basolateral compartment, A is the surface area of the b.End3 monolayers, C is marker's concentration in the apical compartment, and ΔC is the change in solute concentration in the basolateral compartment as a function of time. It is important to note that the transfer of solutes from the apical to the basolateral compartment does not depend on solute concentration, and varies only with the incubation time[9].

Efflux Activity of the P-Glycoprotein Pump

Functional expression of the P-glycoprotein (P-gp) efflux pump by b.End3 cells in single-, bi-, and tri-culture models in layered microfluidic channels was investigated by measuring the apical-to-basolateral (AB) and basolateral-to-apical (BA) permeability of [3H]-Dexamethasone (0.004μM), which is a substrate for the P-gp efflux pump[19]. Briefly, the culture medium in the apical and basolateral channels was replaced with warm PBS (37°C) for washing the cell monolayer twice. PBS solutions were then aspirated and replaced by [3H]-Dexamethasone at the apical (top) compartment for half of the total number of channels and in the basolateral (bottom) compartment in the second half of the channels. All the microfluidic devices were incubated at 37°C, 95% relative humidity,

and 5% CO_2 for 60 minutes. The PBS solution in the receiver compartment of the microfluidic devices was collected and replaced with fresh PBS every 10 minutes for 60 minutes. At the end of the 1 hour incubation time, PBS solutions in both the donor and receiver channels were collected, mixed with 5mL of the liquid scintillation fluid (GMI Inc., Ramsey, MN), and analyzed using the Beckman LS6500 Liquid Scintillation Counter (Beckman Coulter Inc., Brea, CA) to determine the concentration of dexamethasone using a standard calibration curve. We calculated the apical-to-basolateral (AB) and basolateral-to-apical (BA) permeability of [3H]-Dexamethasone using equation 2. We calculated the efflux ratio of dexamethasone in single-, bi-, and tri-culture models by dividing the BA permeability by the AB permeability calculated with each model.

Results and Discussion

Viability and Morphology of b.End3 Cells

We designed the layered microfluidic channels to have an elongated rectangular shape (W = 2mm; L = 4cm; H = 200μm) to mimic small blood vessels and guide the growth of bEnd.3 cells along the channel axis, which has been shown to enhance endothelial cell-cell contact, differentiation, and formation of tight junctions[20, 21]. Using the live/dead assay, we investigated the viability of bEnd.3 cells, pericytes, and astrocytes organized in bi- and tri-culture models. Fluorescent images of the bi-culture **(Figure S1, Supplementary Data)** and the tri-culture model **(Figure S2, Supplementary Data)** show live bEnd.3 cells, pericytes, and astrocytes. Representative images of the tri-culture model confirm the viability of bEnd.3 cells, pericytes, and astrocytes for up to 21 days in culture **(Figure 2B)**. Counting the number of each cell type incorporated in the tri-culture

model shows a statistically significant ($\alpha = 0.05$) increase in the number of viable b.End3 cells from 499±23 cells/mm^2 after 3 days in culture to 627±19 cells/mm^2 after 6 days, which remained constant for 21 days in culture **(Figure 3A)**. The number of viable pericytes steadily increased from 295±15 cells/mm^2 after 3 days to 444±13 cells/mm^2 after 21 days in culture **(Figure 3A)**. Similarly, the number of astrocytes increased from 283±12 cells/mm^2 after 3 days to 369±15 cells/mm^2 after 21 days in culture. These results show the feasibility of co-culturing bEnd.3 cells with pericytes and astrocytes in our layered microfluidic channels and maintaining the viability of cultured cells for up to 21 days in culture.

We measured the angle (θ) between the spindle of b.End3 cells in single, bi-, and tri-culture models and the longitudinal axis of the microfluidic channels as a function of days in culture **(Figure 3B)**. Results show an average angle (θ) of 40°-43° indicating random organization of cultured b.End3 cells after 3 days in culture. However, the angle (θ) gradually declined reaching 21°-25° after 21 days in culture indicating the alignment of b.End3 cells along the length of the microfluidic channel **(Figure 3B)**. This is further supported by the steady decline in the variance (σ^2) in bEnd.3 angle (θ) in relation to the longitudinal axis of the channel in single, bi-, and tri-culture models **(Figure 3C)**. There was an insignificant difference in the angle (θ) of b.End3 cells cultured in single, bi-, and tri-culture models **(Figure 3B)**, which indicates that cell alignment is mediated by channel shape and dimensions and not influenced by co-culture with supporting cells like pericytes and astrocytes. These results are supported by earlier reports showing change in the organization and morphology of endothelial cells in response to the shape and size of the microfluidic channels used for their culture[5, 20-24].

TEER across b.End3 Monolayers

TEER values were measured using embedded Ag/AgCl electrodes in both the top and bottom PDMS layers of the microfluidic channels **(Figure 4A)**[18]. TEER values were resolved by modeling the internal resistance of a cell and the capacitance of the cell membrane in series. Results show that TEER across b.End3 monolayers established as a single culture in microfluidic channels starts at 28 Ohms.cm^2 directly after seeding and gradually increases to 84, 125, and 143 Ohms.cm^2 after 1, 2, and 3 days in culture, respectively **(Figure 4B)**. The b.End3 monolayers established in microfluidic channels maintained an average TEER of ~140 Ohms.cm^2 between days 3 and 21 in culture indicating the viability and high integrity of the formed barrier throughout this culture time **(Figure 4B)**. Similarly, TEER values across co-culture of b.End3 cells and pericytes started at 26 Ohms.cm^2 directly after seeding and gradually increased to 98, 191, and 257 Ohms.cm^2 after 1, 2, and 3 days in culture, respectively, and remained relatively constant for 21 days in culture **(Figure 4B)**. TEER values show that co-culture of b.End3 cells with pericytes increase the integrity of the formed monolayer by 1.8-fold compared to the single culture model **(Figure 4B)**, which is in agreement with previous reports[6, 12, 13]. It is believed that pericytes enhance the integrity of endothelial monolayers through pericytes-bEnd.3 cell contact and secreted chemical factors such as TGFβ[25].

Co-culture of b.End3 cells with pericytes and astrocytes into the tri-culture model increased TEER values from 29 Ohms.cm^2 directly after seeding to 98, 206, and 283 Ohms.cm^2 after 1, 2, and 3 days in culture, respectively **(Figure 4B)**. TEER values remained relatively constant from day 3 up to 21 days in culture. TEER values of the tri-culture model are 2-fold and 1.2-fold higher than those of the single and bi-culture

models, respectively. Results show that incorporating the astrocytes in the co-culture increases the integrity of the formed b.End3 monolayers probably through secreted soluble factors as the height of the lower channel (200μm) does not allow direct contact between the culture astrocytes and the pericytes or bEnd.3 cells. This is not surprising as previous reports showed that astrocytes secrete several chemical factors such as transforming growth factor-β (TGFβ), glial-derived neurotrophic factor (GDNF), and basic fibroblast growth factor (bFGF), which induce BBB properties in endothelial cells *in vitro*[3, 6, 8, 26].

Assessment of Paracellular Permeability across b.End3 Cell Monolayers

We investigated the transport of [14C]-mannitol and [14C]-urea, which are standard paracellular permeability markers, across b.End3 cell monolayers cultured in single , bi-, and tri-culture models to investigate the difference in barrier properties. Results show that permeability of [14C]-mannitol across the single culture of b.End3 cells is 36.4 x 10^{-6} cm/s after 3 days in culture and gradually decreased to 14.6 x 10^{-6} cm/s and 3.4 x 10^{-6} cm/s after 6 and 9 days in culture, respectively **(Figure 5A)**. Permeability of [14C]-mannitol across single b.End3 cell monolayers was 6.3 x 10^{-6}, 3.3 x 10^{-6}, 3.4 x 10^{-6}, and 6.7 x 10^{-6} cm/s after 12, 15, 18, and 21 days in culture, respectively, which indicated the formation of a stable monolayer after 9 days in culture with a modest fluctuation on days 12 and 21 **(Figure 5A)**.

Permeability of [14C]-mannitol across b.End3 cell monolayers in the bi- and tri-culture models was significantly lower than that observed with the single culture model **(Figure 5A)**. Specifically, permeability of [14C]-mannitol across b.End3 cell monolayers

in the bi-culture model started at 1.0 x 10^{-6} cm/s on days 3 and 6 before dropping to 0.5 x 10^{-6} cm/s on day 9 and remaining constant for the rest of the 21 days in culture **(Figure 5A)**. In comparison, permeability of [14C]-mannitol across b.End3 cell monolayers in the tri-culture model was 0.6 x 10^{-6} cm/s on day 3, 0.7 x 10^{-6} cm/s on day 6, 0.4 x 10^{-6} cm/s on days 9, 12, and 15, and 0.3 x 10^{-6} cm/s on days 18 and 21 **(Figure 5A)**. Results show that permeability of [14C]-mannitol across bEnd.3 cell monolayers in the bi-culture model is 6-folds lower than its permeability across the single model, which clearly shows the contribution of co-cultured pericytes to the formation of a more "restrictive" BBB model as described in earlier reports[13]. For example, it has been shown that pericytes-deficient mice mutants demonstrate increased BBB permeability of water and a range of tracer molecules[27]. Pericytes have also been shown to regulate BBB-specific gene expression patterns in endothelial cells and induce polarization of important transport proteins such as P-gp and GLUT-1[6]. The observed 1.7-fold decrease in permeability of [14C]-mannitol across b.End3 cell monolayers in the tri-culture model compared to that observed in the bi-culture model show the positive contribution of astrocytes to the integrity of the formed monolayer. Earlier reports show that astrocytes co-cultured with endothelial cells secrete many neurotrophic factors including TGFβ (MW = 25kDa), bFGF (MW = 18-25kDa), and GDNF (15kDa)[3]. TGFβ is responsible for the growth of endothelial cells and the integrity of microvascular capillaries[28], bFGF mediates angiogenesis and wound healing[29], and GDNF can induce barrier function of endothelial cells and supports its survival[26]. We investigated whether the culture medium in the lower chamber where the astrocytes are seeded show the presence of any proteins in addition to those present in the culture medium. Our preliminary results show an

intense band with an average molecule weight between 25kDa and 50kDa indicating the presence of soluble factors in the culture medium that changes in intensity (i.e. concentration) with the change in the volume of the culture medium **(Figure S4, Supplementary Data)**, which is subject to ongoing proteomics analysis to identify the composition and concentration of these proteins. It is important to note that we did not focus on visualization of tight junctional proteins using confocal microscopy to compare the effect of different culture conditions but rather relied on quantitative assessment of the changes in TEER and [14C]-mannitol permeability in bi- and tri-culture models to deduce the formation of tight junctions between adjacent bEnd.3 endothelial cells and their sensitivity to culture conditions.

We evaluated the permeability of [14C]-urea across bEnd.3 cell monolayers in bi- and tri-culture models to investigate their ability to discriminate between different paracellular permeability markers based on their size. Permeability of [14C]-urea across the bi-culture model started at 1.4 x 10^{-6} cm/s and 1.6 x 10^{-6} cm/s on days 3 and 6, respectively **(Figure 5B)**. Following the same trend for [14C]-mannitol, permeability of [14C]-urea across the bi-culture model dropped to 1.1 x 10^{-6} cm/s on day 9 and remained relatively constant till day 21 in culture. Results clearly show a 0.5- to 2-folds increase in the permeability of [14C]-urea compared to that of [14C]-mannitol on similar days in culture, which indicate the size selectivity of the bi-culture model. Permeability of [14C]-urea across the tri-culture model followed a similar trend to that observed in the bi-culture model **(Figure 5B)**. Further, there was a 2-fold increase in the permeability of [14C]-urea compared to that of [14C]-mannitol on similar days in culture confirming the size selectivity of the tri-culture model. The observed size selectivity of bi- and tri-culture

models coupled with the higher TEER values indicate the formation of restrictive tight junctions between adjacent b.End3 endothelial cells, which is a key characteristic of the BBB *in vivo*[1, 4]. This is supported by the reported permeability of mannitol and urea *in vivo* to be 0.2 x 10^{-6} cm/s[6, 30] and 0.6 x 10^{-6} cm/s[6, 31], respectively.

Porosity of b.End3 Cell Monolayers

The observed difference in permeability of [14C]-mannitol and [14C]-urea across b.End3 monolayers in the bi- and tri-culture models indicate the formation of "restrictive" barriers that can discriminate between diffusing molecules based on their size. By modeling the intercellular space between adjacent endothelial cells as water-filled channels, we calculated the radius (R) of the pores of the tight junctions using the following Renkin function equation:

$$F\left(\frac{r}{R}\right) = (1 - \frac{r}{R})^2[1 - 2.104\left(\frac{r}{R}\right) + 2.09\left(\frac{r}{R}\right)^3 - 0.95\left(\frac{r}{R}\right)^5]$$ ---------- Equation 3

Where the Renkin function F($\frac{r}{R}$) mathematically describes the relationship between the radius of the molecule (r) and the pore radius of the tight junction (R).

The following flux equation provides a relationship between the permeability (P) of a diffusing marker molecule and the Renkin function [$F\left(\frac{r}{R}\right)$].

$$P = \frac{\epsilon D F(\frac{r}{R})}{\delta}$$ ---------- Equation 4

where ϵ is the porosity of the b.End3 monolayer, D is the diffusion coefficient of the evaluated marker molecule, and δ is the distance traversed by the marker molecule down a concentration gradient[32]. We used the diffusion coefficients (D) of mannitol (9.65 x 10-6 cm/s) and urea (13.8 x 10-6 cm/s) with our permeability results **(Figure 5, Panels A&B)**

to solve the equation for the Renkin function $[F\left(\frac{r}{R}\right)]$ and $\frac{\epsilon}{\delta}$ at different time points. We used Matlab R2009a to solve the $[F\left(\frac{r}{R}\right)]$ polynomial equation (Equation 3) and obtained R assuming that the radii (r) of mannitol and urea are 0.34nm[33] and 0.26nm[33, 34], respectively.

Results show that the average radius of the tight junction pores (R) for b.End3 cell monolayers cultured as a single model starting at 46.1 nm on day 3 and dropping to 31.6 nm after 21 days in culture **(Figure 5C)**. The radius of the tight junctions pores (R) for b.End3 cell monolayers in the bi-culture model started at 7.1 nm (day 3) and 7.9 nm (day 6) before dropping to 2.1 nm, 2.7 nm, 3.0 nm, 2.2 nm, and 2.9 nm on days 9, 12, 15, 18, and 21, respectively **(Figure 5C)**. In comparison, the radius of the tight junctions pores (R) for b.End3 cell monolayers in the tri-culture model gradually declined from 2.4 nm (day 3) to 2.1 nm (day 6), 1.6 nm (day 9), 1.7 nm (day 12), 1.6 nm (day 15), and 1.2 nm (days 18 & 21) **(Figure 5C)**. Results show a statically significant (*** indicates α = 0.005; * indicates α = 0.05) decrease in the porosity to the tri-culture model compared to the bi-culture one and confirms the formation of a restrictive barrier throughout the days in culture **(Figure 5C)**. It is important to note that porosity (R = 1.2 + 0.1 nm) of the bEnd.3 cell monolayers in the tri-culture model after 18 days in culture is similar to the reported porosity of the BBB observed *in vivo* (R = 0.8 nm)[35, 36]

Effect of Channel Height on Barrier Properties of b.End3 Monolayers

Earlier reports showed a positive effect of the soluble factors (e.g. TGFβ, bFGF, GDNF) secreted by the pericytes and astrocytes co-cultured with endothelial cells on the integrity of the formed BBB model *in vitro*[3]. This effect was dramatically reduced or

reversed when these factors were not present according to previous studies[3, 26, 29]. Our preliminary results show the presence of soluble factors in the medium collected from the lower channel of the tri-culture model after 21 days in culture **(Figure S4, Supplementary Data)**. We hypothesized that these factors contribute to the observed increase in TEER values, lower permeability of mannitol and urea, and smaller pore size of the tri-culture model compared to the bi-culture one. To test this hypothesis, we increased the height of the lower channel from 200µm to 600µm and 1,000µm while keeping the rest of the channel dimensions constant, which increased the volume of the culture medium in the lower channel from 17µl to 51µl, and 85µl, respectively. We measured the TEER and permeability of [14C]-mannitol across bEnd.3 cell monolayers in the tri-culture model established in the new channels with modified heights. Results show that TEER values in modified lower channels (H = 0.6mm and H = 1mm) are similar in earlier days in culture (days 1-4) **(Figure 6A)**. However, there was a statistically significant ($\alpha = 0.05$) decline in TEER values in modified channels (H = 0.6mm) compared to conventional ones (H = 0.2mm). Similarly, increasing the height of the lower channel to 1.0mm statistically ($\alpha = 0.05$) decreased the recorded TEER values starting day 4 compared to the channel with a height of 0.6mm **(Figure 6A)**.

The observed changes in TEER values were echoed by the calculated permeability of [14C]-mannitol across bEnd.3 cell monolayers in the tri-culture model established in the channels with modified heights **(Figure 6B)**. Specifically, increasing the height of the lower channel to 1mm caused a statistically significant (* indicates $\alpha = 0.05$ and ** indicates $\alpha = 0.01$) increase in the permeability of [14C]-mannitol compared to that observed in 0.2mm channels on days 9-21 **(Figure 6B)**. Similarly, increasing the height

of the lower channel to 0.6mm increased the permeability of [14C]-mannitol compared to that observed in 0.2mm channels on days 18 and 21. It is important to note that the permeability of [14C]-mannitol across bEnd.3 monolayers of the tri-culture model established in modified channels (H = 1.0mm) matched that observed in bi-culture model (i.e. without astrocytes), which indicates the lost effect of the secreted factors in the lower channel **(Figure 6B)**. This can be attributed to the 5-fold increase in the volume of the culture medium causing dilution of the secreted factors, the increase in distance between the cultured astrocytes on the bottom of the lower channel and the cultured bEnd.3 cells onto the porous membrane, or a combination of both. These results are supported by the observed decrease in the density of protein band representing the soluble factors secreted in the culture medium of the lower channel from 217,441 ± 23,188 for 0.2mm channels to 72,779 ± 25,891 for 1.0mm channels **(Figure S4, Supplementary Data)**. The interplay between the height and volume of the lower channel and the associated effect on the barrier properties of the tri-culture model along with identification of these soluble factors are the focus of ongoing investigations.

Functional Expression of P-Glycoprotein

Since the expression of P-glycoprotein alone cannot positively determine the functionality of the P-gp efflux pump[37-44], a quantitative approach using bi-directional permeability was used, instead of methods that only evaluate the level of expression of proteins such as a western blot or qPCR, to evaluate its functional expression. We measured the apical-to-basolateral (AB) and basoalteral-to-apical (BA) permeability of [3H]-Dexamethasone, which is a substrate for the P-gp efflux pump across b.End3 cell

monolayers in the bi- and tri-culture models. Functional expression of the P-gp on the apical side of b.End3 cells would decrease dexamethasone's AB permeability and increase its BA permeability **(Figure 7, Panels A&B)**. Therefore, we calculated dexamethasone's Efflux Ratio (ER)[9] across b.End3 cell monolayers using the following equation.

$$ER = \frac{Permeability_{BA}}{Permeability_{AB}}$$ ---------- Equation 5

Results show that AB permeability of dexamethasone gradually decreased from 5.1 x 10^{-6} cm/s on day 3 to 2.9 x 10^{-6} cm/s on day 21 **(Figure 7A)**. In parallel, BA permeability of dexamethasone gradually increased from 6.2 x 10^{-6} cm/s on day 3 to 8.2 x 10^{-6} cm/s on day 21 **(Figure 7A)**. This permeability profile led to an ER of 1.2 on day 3, which gradually increased reached 2.8 on day 21 indicating the increase in functional expression of the P-gp efflux pump in the bi-culture model with the increase in culture time **(Figure 7C)**. Similarly, dexamethasone's AB permeability across the tri-culture model gradually decreased from 4.7 x 10^{-6} cm/s on day 3 to 2.1 x 10^{-6} cm/s on day 21 while the BA permeability gradually increased from 7.3 x 10^{-6} cm/s on day 3 to 10 x 10^{-6} cm/s on day 21 **(Figure 7B)**. The calculated ER for the tri-culture model gradually increased from 1.6 on day 3 to 4.8 on day 21 **(Figure 7C)**. It is interesting to note the statistically higher (* indicates $\alpha = 0.05$ and ** indicates $\alpha = 0.01$) ER with the tri-culture model compared to the bi-culture one starting from day 12, which indicates enhanced P-gp activity in the tri-culture model **(Figure 7C)**.

Conclusions

We report the successful co-culture of brain endothelial cells (b.End3) with pericytes alone or in combination with astrocytes in layered microfluidic channels to establish bi- and tri-culture models of the blood-brain barrier, which exhibits different degrees of "restrictiveness" indicated by their high TEER values and low permeability of [14C]-mannitol and [14C]-urea. Both the bi- and tri-culture models exhibited functional expression of the P-gp efflux pump, which increased with the increase in number of days in culture. Based on the similarity in mannitol permeability across b.End3 cell monolayers in the tri-culture model to reported mannitol permeability across the BBB *in vivo* and the high functional expression of the P-gp efflux pump, we believe that the tri-culture model described in this report represents a 3D *in vitro* model of the BBB that closely mimics its restrictive nature observed *in vivo*.

Acknowledgement

This research was supported in part by the University of Michigan Microfluidics in Biomedical Sciences Training Program, and Rackham Merit Fellowship. We would like to thank Dr. Anuska Andjelkovic-Zochowska for her technical input and discussion of the reported results.

Supporting Information

Additional fluorescent images of bEnd.3 cells, pericytes, and astrocytes in the bi- and tri-culture system plus a western blot of the culture medium in the tri-culture model are supplied in the Supporting Information.

References

1. Dermietzel, R.; Spray, D. C.; Nedergaard, M., *Blood-Brain Barrier: From Ontogeny to Artificial Interfaces*. WILEY-VCH: Weinheim, Germany, 2006; Vol. 2.

2. Pardridge, W. M. Blood-Brain Barrier Drug Targeting: The Future of Brain Drug Development. *Mol. Interventions* **2003,** *3*, (2), 90-105.

3. Abbott, N. J.; Ronnback, L.; Hansson, E. Astrocyte-endothelial interactions at the blood-brain barrier. *Nat. Rev. Neurosci.* **2006,** *7*, 41-53.

4. Pardridge, W. M. Why is the global CNS pharmaceutical market so under-penetrated? *DDT* **2002,** *7*, (1), 5-7.

5. van der Meer, A. D.; Orlova, V. V.; ten Dijke, P.; van den Berg, A.; Mummery, C. L. Three-dimensional co-cultures of human endothelial cells and embryonic stem cell-derived pericytes inside a microfluidic device. *Lab Chip* **2013,** *13*, (18), 3562-3568.

6. Deli, M. A.; Abraham, C. S.; Kataoka, Y.; Niwa, M. Permeability Studies on *In Vitro* Blood-Brain Barrier Models: Physiology, Pathology, and Pharmacology. *Cell. Mol. Neurobiol.* **2004,** *25*, (1), 59-127.

7. Omidi, Y.; Campbell, L.; Barar, J.; Connell, D.; Akhtar, S.; Gumbleton, M. Evaluation of the immortalised mouse brain capillary endothelial cell line, b.End3, as an *in vitro* blood-brain barrier model for drug uptake and transport studies. *Brain Res.* **2003,** *990*, 95-112.

8. Abbott, N. J. Astrocyte-endothelial interactions and blood-brain barrier permeability. *J. Anat.* **2002,** *200*, (6), 629-638.

9. Cucullo, L.; Couraud, P.-O.; Weksler, B.; Romero, I.-A.; Hossain, M.; Rapp, E.; Janigro, D. Immortalized human brain endothelial cells and flow-based vascular

modeling: a marriage of convenience for rational neurovascular studies. *J. Cereb. Blood Flow Metab.* **2008,** *28*, 312-328.

10. Booth, R.; Kim, H. Characterization of a microfluidic *in vitro* model of the blood-brain barrier (uBBB). *Lab Chip* **2012,** *12*, 1784-1792.

11. Prabhakarpandian, B.; Shen, M.-C.; Nichols, J. B.; Mills, I. R.; Sidoryk-Wegrzynowicz, M.; Aschner, M.; Pant, K. SyM-BBB: a microfluidic blood brain barrier model. *Lab Chip* **2013,** *13*, 1093-1101.

12. Allt, G.; Lawrenson, J. G. Pericytes: Cell Biology and Pathology. *Cells Tissues Organs* **2001,** *169*, (1), 1-11.

13. Armulik, A.; Genove, G.; Betsholtz, C. Pericytes: developmental, physiological, and pathological perspectives, problems, and promises. *Dev. Cell* **2011,** *21*, (2), 193-215.

14. Betsholtz, C.; Lindblom, P.; Gerhardt, H. Role of pericytes in vascular morphogenesis. *Mechanisms of Angiogenesis* **2005,** *94*, (115-125).

15. Lai, C.-H.; Kuo, K.-H. The critical component to establish in vitro BBB model: Pericyte. *Brain Res. Rev.* **2005,** *50*, 258-265.

16. Pietro, A. D.; Dayan, G.; COnseil, G.; Steinfels, E.; Krell, T.; Trompier, D.; Baubichon-Cortay, H.; Jault, J.-M. P-glycoprotein-mediated resistance to chemotherapy in cancer cells: using recombinant cytosolic domains to establish structure-function relationships. *Braz. J. Med. Biol. Res.* **1999,** *32*, 925-939.

17. Chueh, B.-h.; Huh, D.; Kyrtsos, C. R.; Houssin, T.; Futai, N.; Takayama, S. Leakage-Free Bonding of Porous Membranes into Layered Microfluidic Array Systems. *Anal. Chem.* **2007,** *79*, (9), 3504-3508.

18. Douville, N. J.; Tung, Y.-C.; Li, R.; Wang, J. D.; El-Sayed, M. E. H.; Takayama, S. Fabrication of Two-Layered Channel System with Embedded Electrodes to Measure Resistance Across Epithelial and Endothelial Barriers. *Anal. Chem.* **2010,** *82*, (6), 2505-2511.

19. Ueda, K.; Okamura, N.; Hirai, M.; Tanigawara, Y.; Saeki, T.; Kioka, N.; Komano, T.; Hori, R. Human P-glycoprotein Transports Cortisol, Aldosterone, and Dexamethasone, but Not Progesterone. *J. Biol. Chem.* **1992,** *267*, (34), 24248-24252.

20. Huang, S.; Ingber, D. E. Shape-Dependent Control of Cell Growth, Differentiation, and Apoptosis: Switching between Attractors in Cell Regulatory Networks. *Exp. Cell Res.* **2000,** *261*, 91-103.

21. Huang, Z.; Li, X.; Martins-Green, M.; Liu, Y. Microfabrication of cylindrical microfluidic channel networks for microvascular research. *Biomed. Microdevices* **2012,** *14*, (5), 873-883.

22. Baker, B. M.; Trappmann, B.; Stapleton, S. C.; Toro, E.; Chen, C. S. Microfluidics embedded within extracellular matrix to define vascular architectures and pattern diffusive gradients. *Lab Chip* **2013,** *13*, (16), 3246-3252.

23. Tung, C.-k.; Krupa, O.; Apaydin, E.; Liou, J.-J.; Diaz-Santana, A.; Kim, B. J.; Wu, M. A contact line pinning based microfluidic platform for modelling physiological flows. *Lab Chip* **2013,** *13*, (19), 3876-3885.

24. Wang, X.-Y.; Jin, Z.-H.; Gan, B.-W.; Lv, S.-W.; Xie, M.; Huang, W.-H. Engineering interconnected 3D vascular networks in hydrogels using molded sodium alginate lattice as the sacrificial template. *Lab Chip* **2014,** *14*, (15), 2709-2716.

25. Cecchelli, R.; Aday, S.; Sevin, E.; Almeida, C.; Culot, M.; Dehouck, L.; Coisne, C.; Engelhardt, B.; Dehouck, M.-P.; Ferreira, L. A Stable and Reproducible Human Blood-Brain Barrier Model Derived from Hematopoietic Stem Cells. *PLOS One* **2014,** *9*, (6).

26. Igarashi, Y.; Utsumi, H.; Chiba, H.; Yamada-Sasamori, Y.; Tobioka, H.; Kamimura, Y.; Furuuchi, K.; Kokai, Y.; Nakagawa, T.; Mori, M.; Sawada, N. Glial Cell Line-Derived Neurotrophic Factor Induces Barrier Function of Endothelial Cells Forming the Blood-Brain Barrier. *Biochem. Biophys. Res. Comm.* **1999,** *261*, (1), 108-112.

27. Armulik, A.; Genove, G.; Mae, M.; Nisancioglu, M. H.; Wallgard, E.; Niaudet, C.; He, L.; Norlin, J.; Lindblom, P.; Strittmatter, K.; Johansson, B. R.; Betsholtz, C. Pericytes regulate the blood-brain barrier. *Nature* **2010,** *468*, 557-561.

28. Dohgu, S.; Takata, F.; Yamauchi, A.; Nakagawa, S.; Egawa, T.; Naito, M.; Tsuruo, T.; Sawada, Y.; Niwa, M.; Kataoka, Y. Brain pericytes contribute to the induction and up-regulation of blood-brain barrier functions through transforming growth factor-β production. *Brain Res.* **2005,** *1038*, (2), 208-215.

29. Nissen, N. N.; Polverini, P. J.; Gamelli, R. L.; DiPietro, L. A. Basic fibroblast growth factor mediates angiogenic activity in early surgical wounds. *Surgery* **1996,** *119*, (4), 457-465.

30. Johanson, C. E. Permeability and Vascularity of the Developing Brain: Cerebellum vs Cerebral Cortex. *Brain Res.* **1980,** *190*, 3-16.

31. Dagenais, C.; Rousselle, C.; Pollack, G. M.; Scherrmann, J.-M. Development of an *In Situ* Mouse Brain Perfusion Model and Its Application to *mdr1a* P-glycoprotein-Deficient Mice. *J. Cereb. Blood Flow Metab.* **2000,** *20*, 381-386.

32. Adson, A.; Raub, T. J.; Burton, P. S.; Barsuhn, C. L.; Hilgers, A. R.; Audus, K. L.; Ho, N. F. H. Quantitative Approaches To Delineate Paracellular Diffusion in Cultured Epithelial Cell Monolayers. *J. Pharm. Sci.* **1994,** *83*, (11), 1529-1536.

33. Ghandehari, H.; Smith, P. L.; Ellens, H.; Yeh, P.-Y.; Kopecek, J. Size-Dependent Permeability of Hydrophilic Probes Across Rabbit Colonic Epithelium. *J. Pharmacol. Exp. Ther.* **1997,** *280*, (2), 747-753.

34. Cussler, E. L., *Diffusion: Mass Transfer in Fluid Systems*. Cambridge University Press: Cambridge, 2009.

35. Tarbell, J. M. Shear stress and the endothelial transport barrier. *Cardiovasc. Res.* **2010,** *87*, (2), 320-330.

36. Thomas, S. A.; Segal, M. B. The transport of the anti-HIV drug, 2',3'-didehydro-3'-deoxythymidine (D4T), across the blood-brain and blood-cerebrospinal fluid barriers. *Br. J. Pharmacol.* **1998,** *125*, 49-54.

37. Bailly, J. D.; Muller, C.; Jaffrezou, J. P.; Dmur, C.; Gassar, G.; Bordier, C.; Laurent, G. Lack of correlation between expression and function of P-glycoprotein in acute myeloid leukemia cell lines. *Leukemia* **1995,** *9*, (5), 799-807.

38. Leith, C. P.; Chen, I. M.; Kopecky, J. J.; Appelbaum, F. R.; Head, D. R.; Godwin, J. E.; Weick, J. K.; Willman, C. L. Correlation of multidrug resistance (MDR1) protein expression with functional dye/drug efflux in acute myeloid leukemia by multiparameter flow cytometry: identification of discordant MDR-/efflux+ and MDR1+/efflux- cases. *Blood* **1995,** *86*, (6), 2329-2342.

39. Moerloose, B. D.; Dhooge, C.; Laureys, G.; Benoit, Y.; Demarche, M.; Devalck, C.; Plantaz, D.; Leroy, J.; Philippe, J. Discrepant flow cytometric expression and

function of P-glycoprotein in neuroblastic tumors. *Cytometry, Part A* **1999,** *37*, (2), 125-132.

40. Moerloose, B. D.; Dhooge, C.; Philippe, J. Discordance of P-glycoprotein expression and function in acute leukemia. *Adv. Exp. Med. Biol.* **1999,** *457*, 107-118.

41. Meaden, E. R.; Hoggard, P. G.; Khoo, S. H.; Back, D. J. Determination of P-gp and MRP1 expression and function in peripheral blood mononuclear cells in vivo. *J. Immunol. Methods* **2002,** *262*, (1-2), 159-165.

42. Yang, Z. H.; Liu, X. D. P-glycoprotein-mediated efflux of phenobarbital at the blood-brain barrier evidence from transport experiments in vitro. *Epilepsy Res.* **2008,** *78*, 40-49.

43. Hakkarainen, J. J.; Rilla, K.; Suhonen, M.; Ruponen, M.; Forsberg, M. M. Re-evaluation of the role of P-glycoprotein in in vitro drug permeability studies with the bovine brain microvessel endothelial cells. *Xenobiotica* **2014,** *44*, (3), 283-294.

44. Tai, L. M.; Reddy, P. S.; Lopez-Ramirez, M. A.; Davies, H. A.; Male, D. K.; Loughlin, A. J.; Romero, I. A. Polarized P-glycoprotein expression by the immortalized human brain endothelial cell line, hCMEC/D3, restricts apical-to-basolateral permeability to rhodamine 123. *Brain Res.* **2009,** *1292*, (14-24).

Figure Caption

Figure 1. A schematic drawing showing the anatomical organization of the endothelial cells, pericytes, and astrocytes, which control the integrity of the blood-brain barrier (BBB) *in vivo*.

Figure 2. (A) The schematic drawing of layered PDMS channels (40mm x 2mm x 0.2mm) sandwiching a polyester membrane (pore size = 400 nm) and the organization of b.End3 endothelial cells, pericyte, and astrocytes in the tri-culture model. (B) Fluorescent images (10x magnification) of viable b.End3 endothelial cells, pericytes, and astrocytes co-cultured in the tri-culture model after 3 and 21 days in culture.

Figure 3. (A) The change in number of bEnd3 endothelial cells, pericytes, and astrocytes in the tri-culture model as a function of days in culture. The change in (B) angle (θ) and (C) variance of angle (σ^2) of b.End3 cells cultured in single, bi-, and tri-culture models as a function of days in culture.

Figure 4. (A) A schematic drawing showing the design of the layered microfluidic channels and the equivalent circuit model. Ag/AgCl recording electrodes are embedded on opposing sides bEnd.3 cells cultured on a polyester porous membrane. Electrical current has two parallel paths through the confluent cell monolayer. The transcellular path can be modeled by the internal resistance of a cell (RI) in series with the capacitance of the cell membranes (CM). The paracellular path is modeled by the resistor (RE) and represents the trans-endothelial electrical resistance (TEER) of the experiment [18]. (B) The

TEER across b.End3 monolayers in single, bi-, and tri-culture models at different days in culture. The * ($p<0.05$), ** ($p<0.01$), and *** ($p<0.005$) indicate statistically higher TEER in the bi-culture model compared to the single culture model. The + ($p<0.05$), ++ ($p<0.01$), and +++ ($p<0.005$) indicate statistically higher TEER in the tri-culture model compared to the bi-culture one at similar time points.

Figure 5. (A) Permeability of [14C]-mannitol across b.End3 monolayers in single, bi-, and tri-culture models at different days in culture. The inset figure show the permeability of [14C]-mannitol in the bi- and tri-culture model. (B) Permeability of [14C]-urea across b.End3 monolayers in bi- and tri-culture models at different days in culture. The * ($p<0.05$), ** ($p<0.01$), and *** ($p<0.005$) indicate a statistically lower permeability between connected bars (dashed lines) at similar time points. (C) Radius of the pores of the tight junctions (R) in b.End3 monolayers in single, bi-, and tri-culture models. The * ($p<0.05$), ** ($p<0.01$), and *** ($p<0.005$) indicate a statistically lower radius (R) of the pores in the tight junctions of connected bars (dashed lines) at similar time points.

Figure 6. (A) The TEER across b.End3 cell monolayers in the tri-culture model with modified height (H = 0.2mm, 0.6mm, or 1.0mm) for the lower microfluidic channel as a function of days in culture. (B) Permeability of [14C]-mannitol across b.End3 monolayers in the bi-culture and tri-culture (H of lower channel = 0.2mm, 0.6mm, or 1.0mm) models at different days in culture where * ($p<0.05$) and ** ($p<0.01$) indicate a statistically lower permeability between connected bars (dashed lines) at similar time points.

Figure 7. Apical-to-basolateral (AB) and basolateral-to-apical (BA) permeability of [3H]-dexamethasone across b.End3 monolayers cultured in bi-culture (A) and tri-culture (B) models at different days in culture. The * ($p<0.05$), ** ($p<0.01$), and *** ($p<0.005$) indicate statistical difference in dexamethasone AB and BA permeability. (C) Comparing the ER of [3H]-dexamethasone in b.End3 monolayers established in the bi- and tri-culture models at different days in culture. The * ($p<0.05$) and ** ($p<0.01$) indicate a statistically higher ER in the tri-culture model compared to the bi-culture one at the same time points.

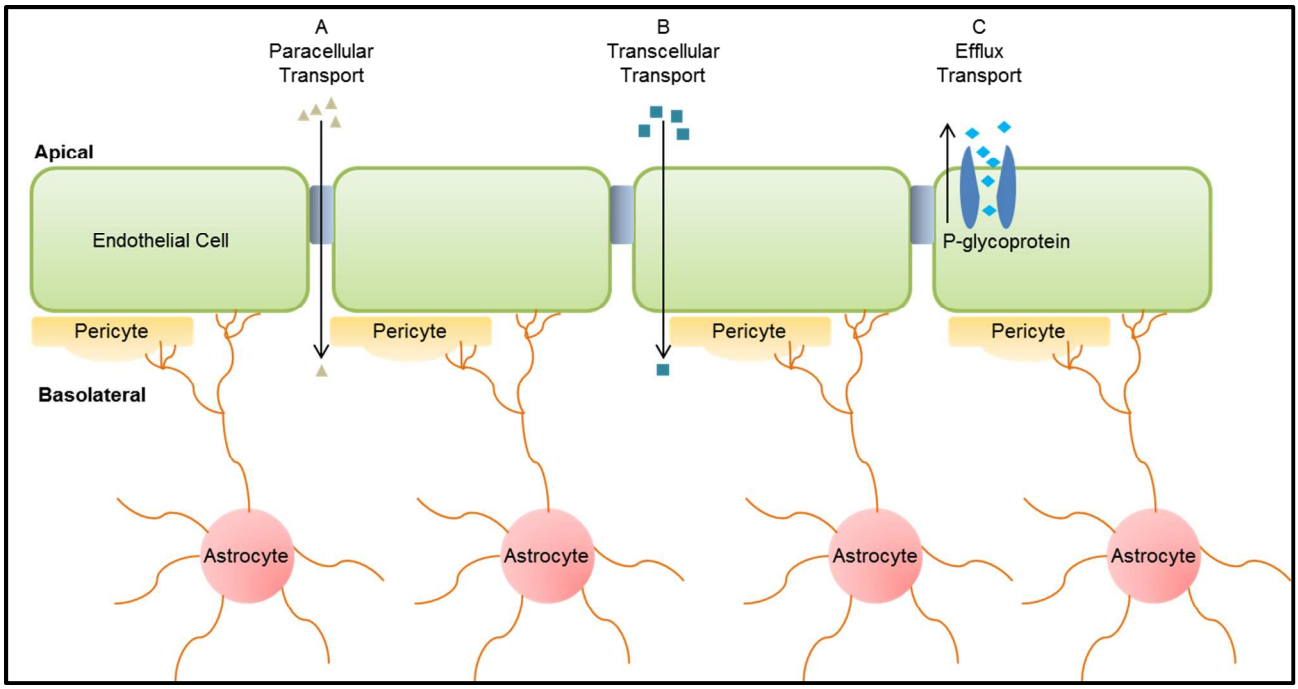
A
Paracellular
Transport
B
Transcellular
Transport
C
Efflux
Transport
Apical
Endothelial Cell
P-glycoprotein
Pericyte
Pericyte
Pericyte
Pericyte
Basolateral
Astrocyte
Astrocyte
Astrocyte
Astrocyte

Figure 1.

(A)

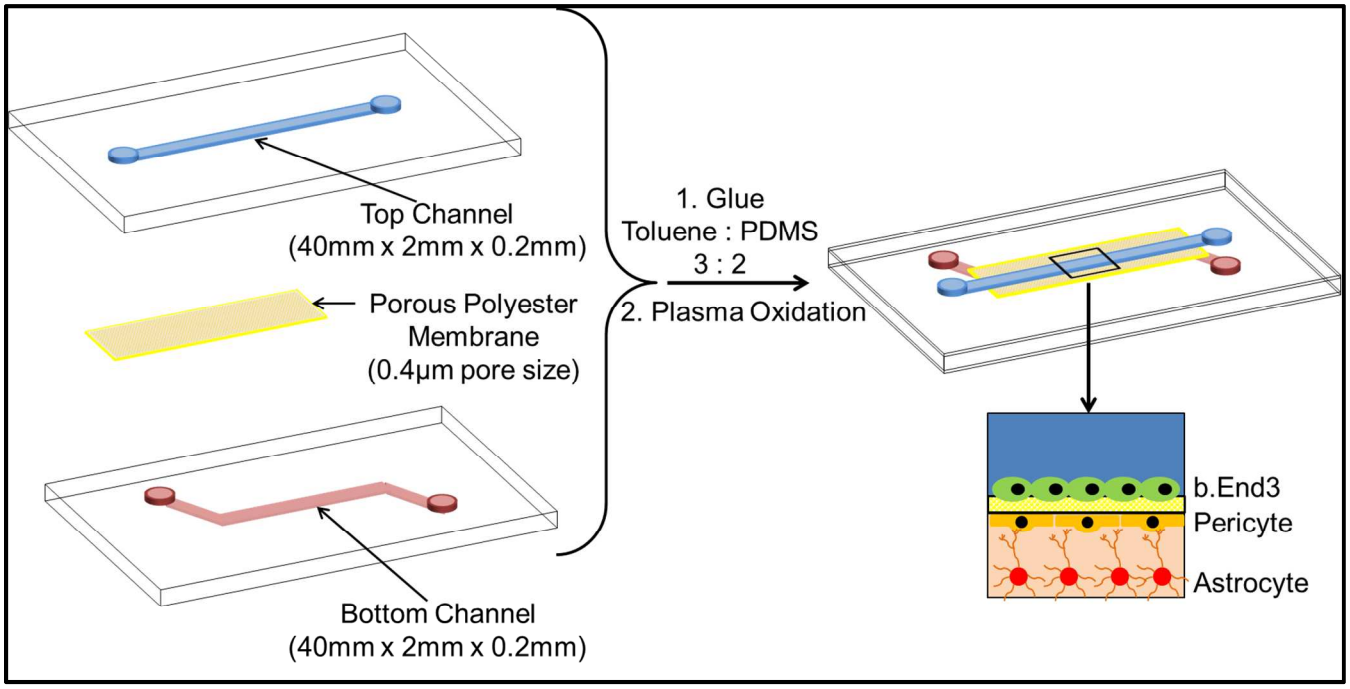
Top Channel
(40mm x 2mm x 0.2mm)
Porous Polyester
Membrane
(0.4μm pore size)
Bottom Channel
(40mm x 2mm x 0.2mm)
1. Glue
Toluene : PDMS
3 : 2
2. Plasma Oxidation
b.End3
Pericyte
Astrocyte

(B)

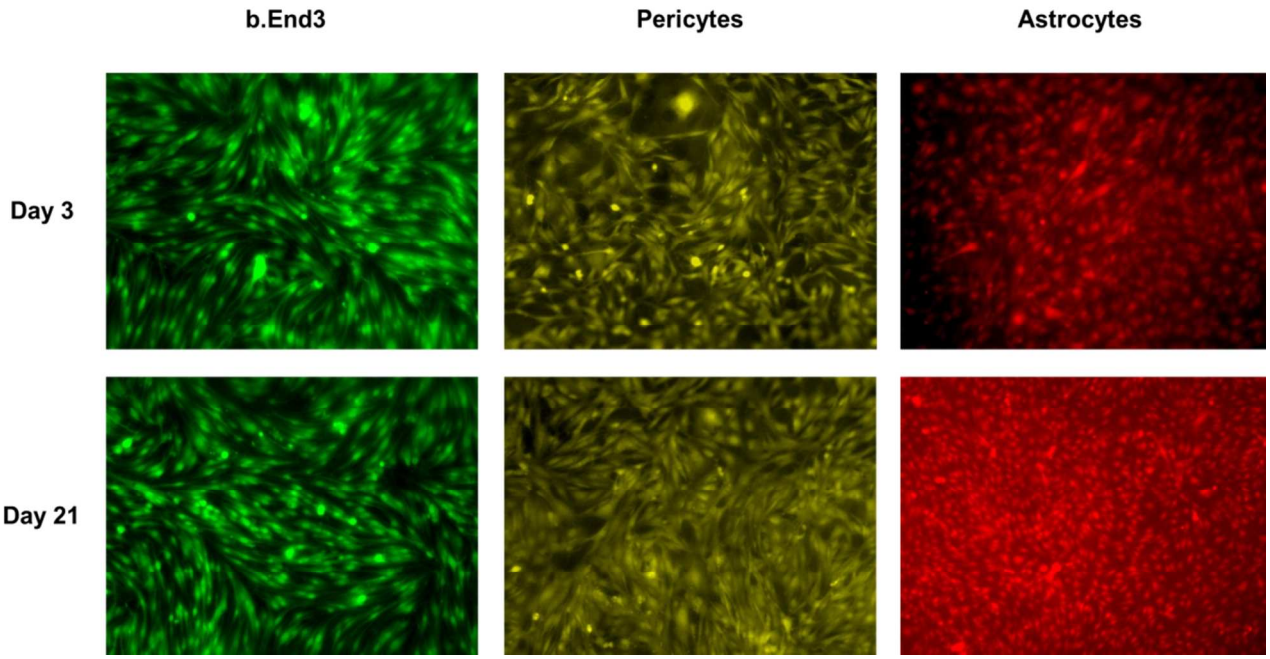
b.End3
Pericytes
Astrocytes
Day 3
Day 21

Figure 2.

(A)

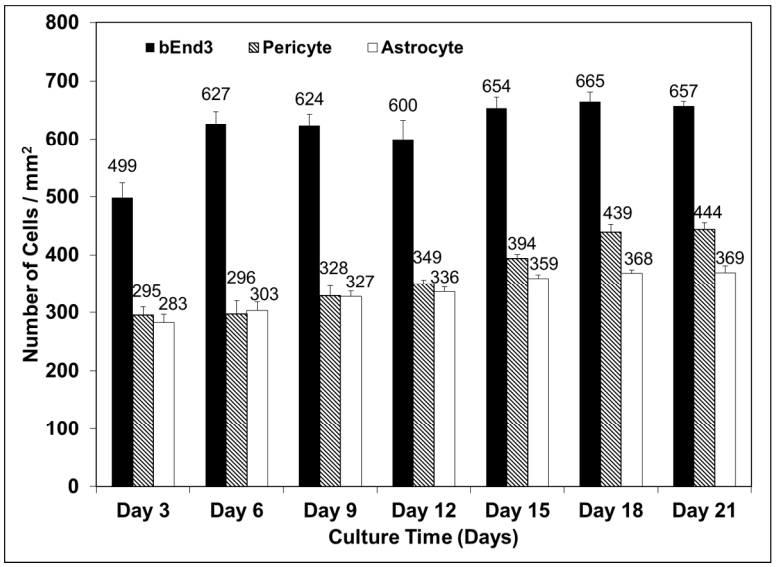
bEnd3
Pericyte
Astrocyte
Number of Cells / mm2
800
700
600
500
400
300
200
100
0
499
295
283
627
296
303
624
328
327
600
349
336
654
394
359
665
439
368
657
444
369
Day 3
Day 6
Day 9
Day 12
Day 15
Day 18
Day 21
Culture Time (Days)

(B)

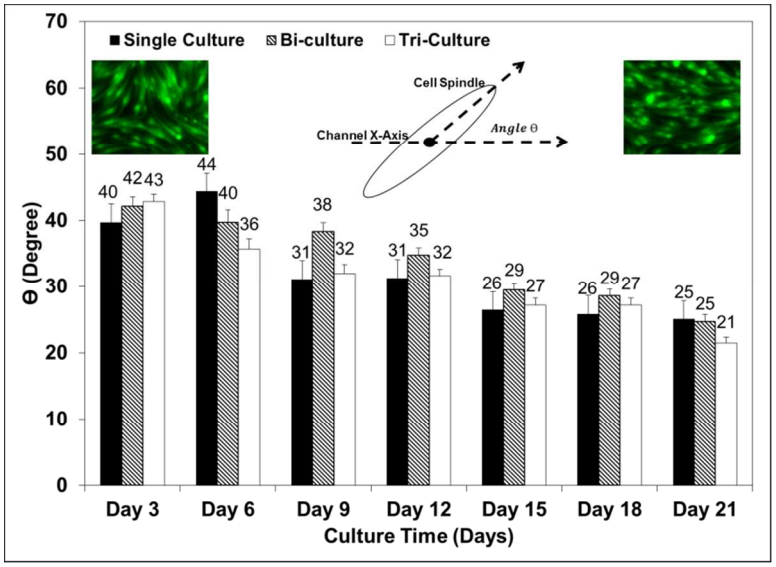
Single Culture
Bi-culture
Tri-Culture
Cell Spindle
Channel X-Axis
Angle θ
Θ (Degree)
70
60
50
40
30
20
10
0
40
42
43
44
40
36
31
38
32
31
35
32
26
29
27
26
29
27
25
25
21
Day 3
Day 6
Day 9
Day 12
Day 15
Day 18
Day 21
Culture Time (Days)

(C)

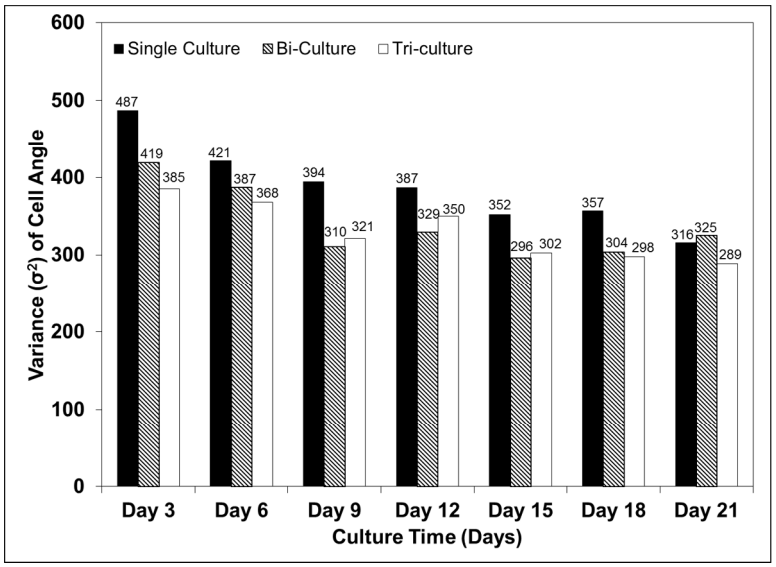
Single Culture
Bi-Culture
Tri-culture
Variance (σ^2) of Cell Angle
600
500
400
300
200
100
0
487
419
385
421
387
368
394
310
321
387
329
350
352
296
302
357
304
298
316
325
289
Day 3
Day 6
Day 9
Day 12
Day 15
Day 18
Day 21
Culture Time (Days)

Figure 3.

(A)

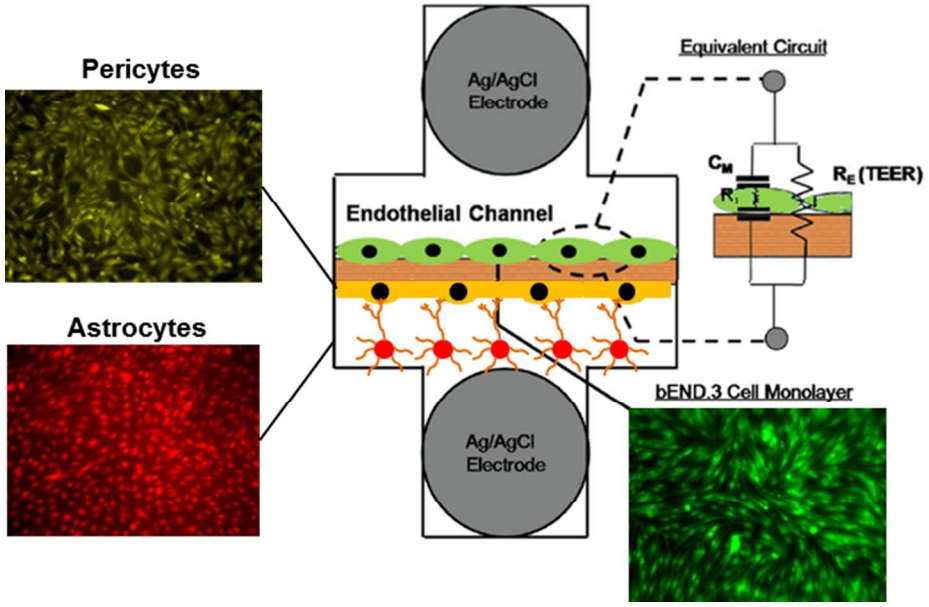
Pericytes
Astrocytes
Ag/AgCl Electrode
Endothelial Channel
Ag/AgCl Electrode
Equivalent Circuit
C_M
R_E (TEER)
bEND.3 Cell Monolayer

(B)

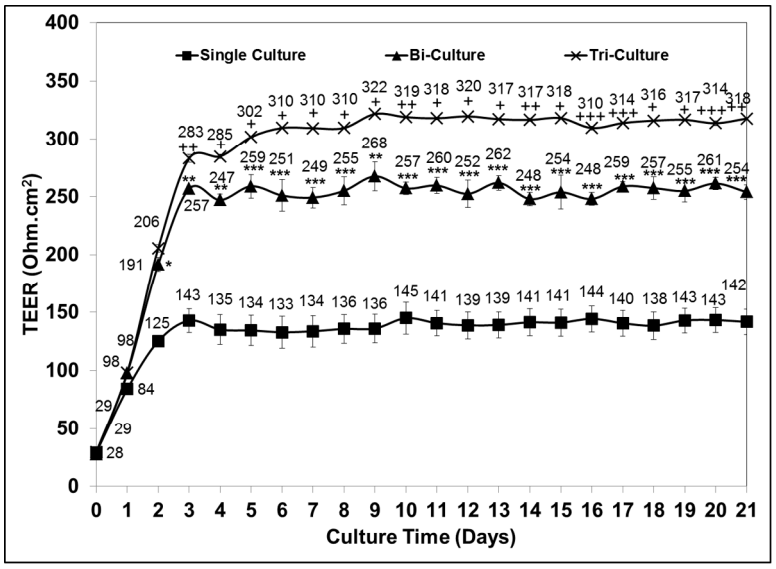
Single Culture
Bi-Culture
Tri-Culture
TEER (Ohm.cm²)
Culture Time (Days)

Figure 4.

(A)

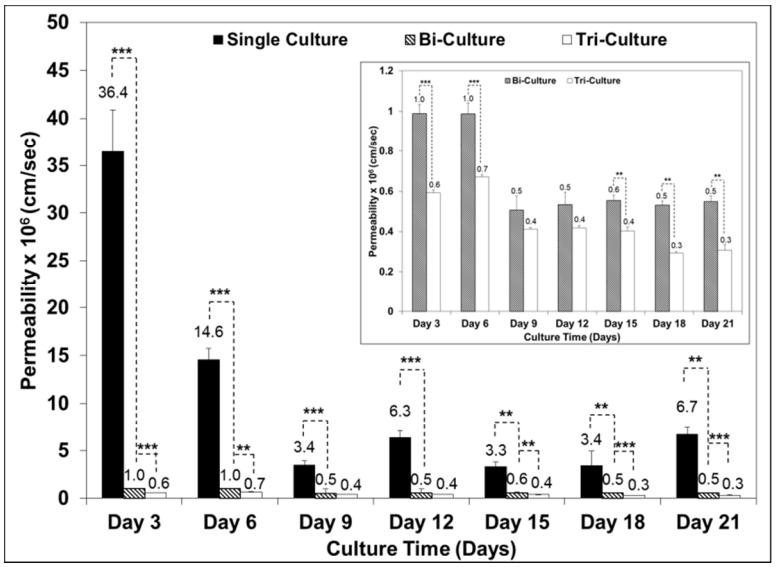
Single Culture
Bi-Culture
Tri-Culture
Permeability x 10^6 (cm/sec)
Culture Time (Days)
Day 3
Day 6
Day 9
Day 12
Day 15
Day 18
Day 21
36.4
1.0
0.6
14.6
1.0
0.7
3.4
0.5
0.4
6.3
0.5
0.4
3.3
0.6
0.4
3.4
0.5
0.3
6.7
0.5
0.3
Permeability x 10^6 (cm/sec)
Culture Time (Days)

(B)

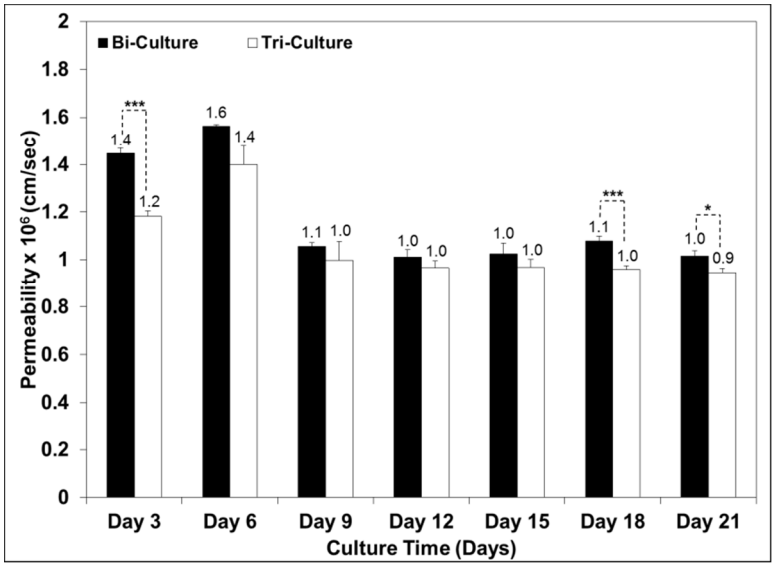
Bi-Culture
Tri-Culture
Permeability x 10^6 (cm/sec)
Culture Time (Days)
Day 3
Day 6
Day 9
Day 12
Day 15
Day 18
Day 21
1.4
1.2
1.6
1.4
1.1
1.0
1.0
1.0
1.0
1.0
1.1
1.0
1.0
0.9

(C)

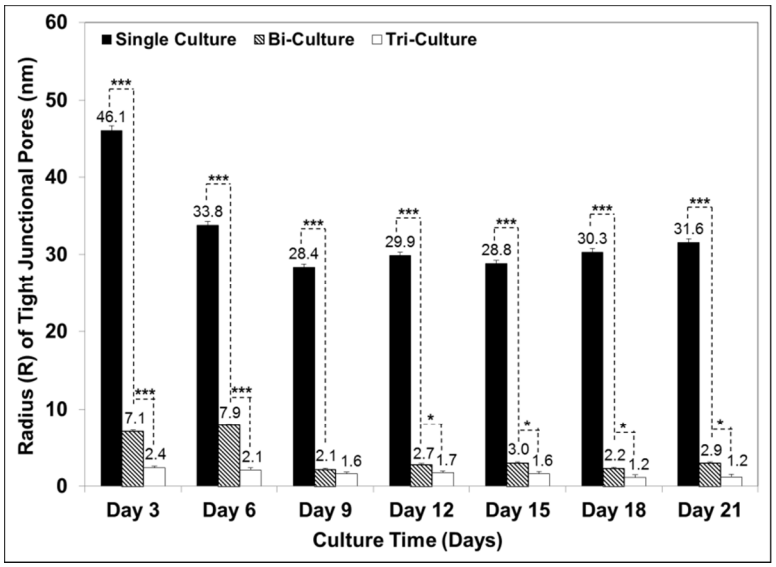
Single Culture
Bi-Culture
Tri-Culture
Radius (R) of Tight Junctional Pores (nm)
60
50
40
30
20
10
0
46.1
7.1
2.4
33.8
7.9
2.1
28.4
2.1
1.6
29.9
2.7
1.7
28.8
3.0
1.6
30.3
2.2
1.2
31.6
2.9
1.2
***
*
Day 3
Day 6
Day 9
Day 12
Day 15
Day 18
Day 21
Culture Time (Days)

Figure 5.

(A)

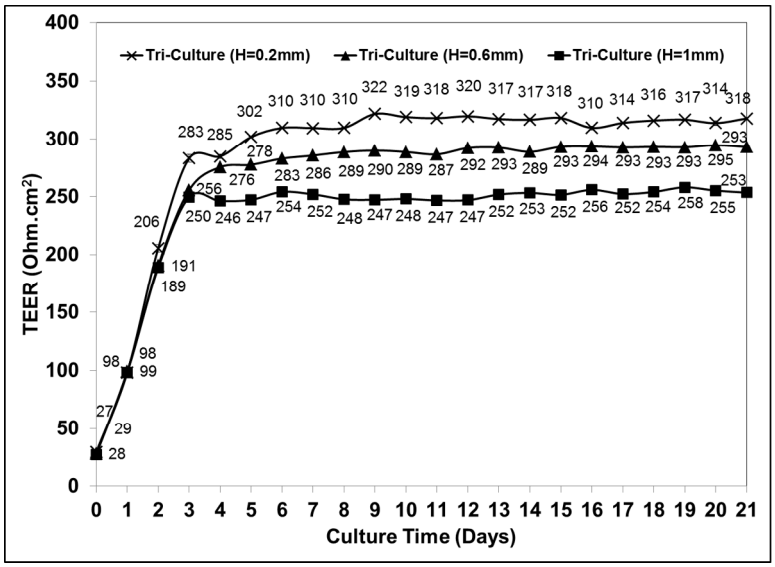
Tri-Culture (H=0.2mm)
Tri-Culture (H=0.6mm)
Tri-Culture (H=1mm)
TEER (Ohm.cm²)
Culture Time (Days)

(B)

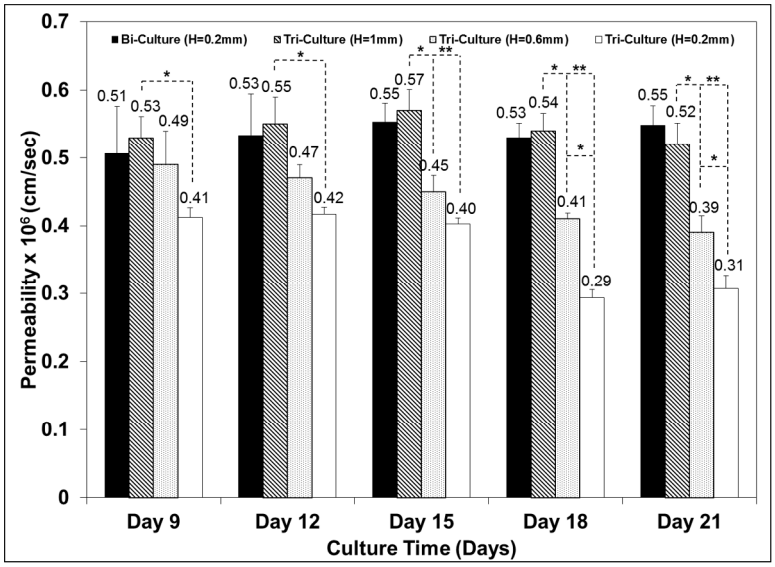
Bi-Culture (H=0.2mm)
Tri-Culture (H=1mm)
Tri-Culture (H=0.6mm)
Tri-Culture (H=0.2mm)
Permeability x 10⁶ (cm/sec)
Day 9
Day 12
Day 15
Day 18
Day 21
Culture Time (Days)

Figure 6.

(A)

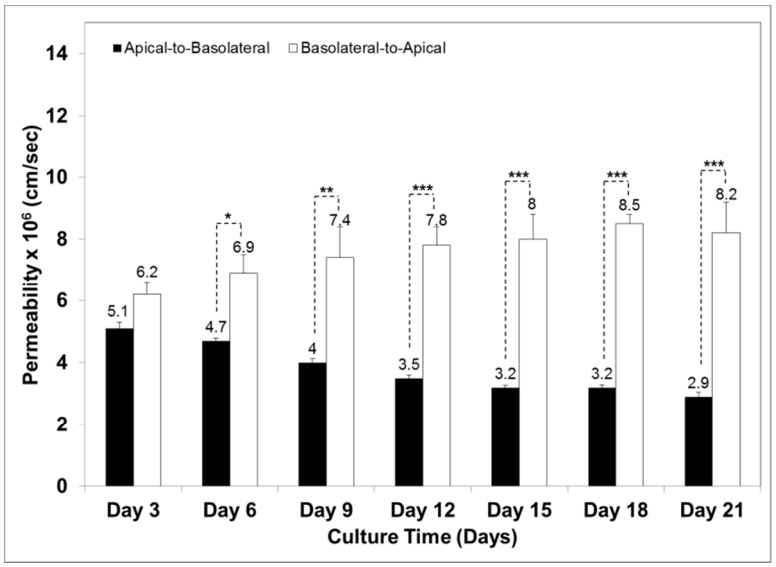
Apical-to-Basolateral
Basolateral-to-Apical
Permeability x 10⁶ (cm/sec)
Culture Time (Days)
Day 3
Day 6
Day 9
Day 12
Day 15
Day 18
Day 21
5.1
6.2
4.7
6.9
4
7.4
3.5
7.8
3.2
8
3.2
8.5
2.9
8.2

(B)

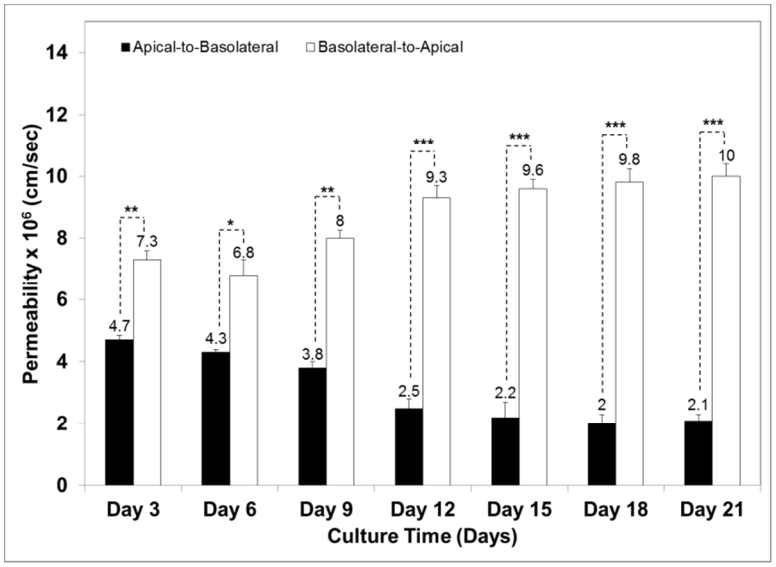
Apical-to-Basolateral
Basolateral-to-Apical
Permeability x 10⁶ (cm/sec)
Culture Time (Days)
Day 3
Day 6
Day 9
Day 12
Day 15
Day 18
Day 21
4.7
7.3
4.3
6.8
3.8
8
2.5
9.3
2.2
9.6
2
9.8
2.1
10

(C)

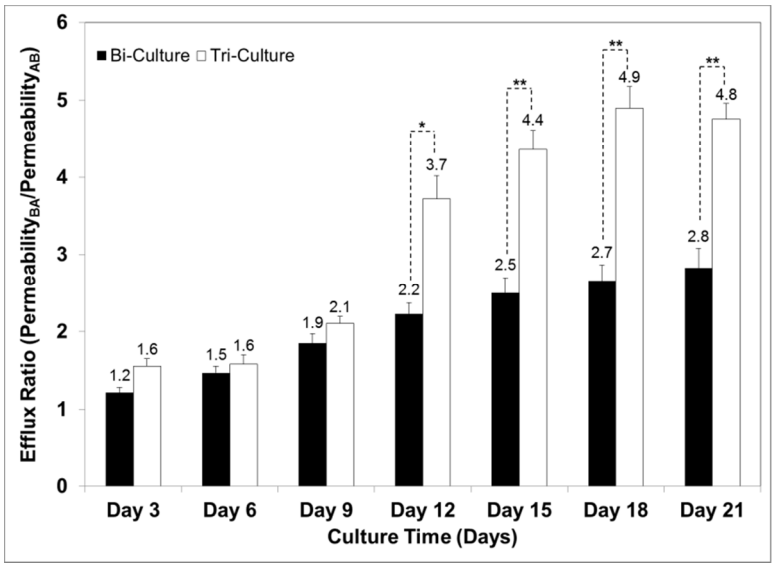
Efflux Ratio (Permeability$_{BA}$/Permeability$_{AB}$)
Bi-Culture
Tri-Culture
0
1
2
3
4
5
6
1.2
1.6
1.5
1.6
1.9
2.1
2.2
3.7
2.5
4.4
2.7
4.9
2.8
4.8
*
**
**
**
Day 3
Day 6
Day 9
Day 12
Day 15
Day 18
Day 21
Culture Time (Days)

Figure 7.